



HAL
open science

Targeted Thermal and Electrical Properties of Rubber Materials for HVDC Cable Accessories

Thi Thu Nga Vu, Séverine Le Roy, G. Teyssedre

► **To cite this version:**

Thi Thu Nga Vu, Séverine Le Roy, G. Teyssedre. Targeted Thermal and Electrical Properties of Rubber Materials for HVDC Cable Accessories. IEEE 4th International Conference on Dielectrics (ICD 2022), Jul 2022, Palermo, Italy. pp.53-56, 10.1109/ICD53806.2022.9863471 . hal-03784544

HAL Id: hal-03784544

<https://hal.science/hal-03784544>

Submitted on 23 Sep 2022

HAL is a multi-disciplinary open access archive for the deposit and dissemination of scientific research documents, whether they are published or not. The documents may come from teaching and research institutions in France or abroad, or from public or private research centers.

L'archive ouverte pluridisciplinaire **HAL**, est destinée au dépôt et à la diffusion de documents scientifiques de niveau recherche, publiés ou non, émanant des établissements d'enseignement et de recherche français ou étrangers, des laboratoires publics ou privés.

Targeted Thermal and Electrical Properties of Rubber Materials for HVDC Cable Accessories

T.T.N. Vu¹, S. Le Roy², G. Teyssedre²

¹Electric Power University, Hanoi, Vietnam

²LAPLACE, Université de Toulouse, CNRS, INPT, UPS, Toulouse, France
gilbert.teyssedre@laplace.univ-tlse.fr

Abstract- The choice of rubber material used in DC accessories as joints is a delicate task as the stresses to support resort to both capacitive and resistive distribution, and the thermal gradient set during cable operation further modifies the stress distribution. Field distributions in a model HVDC joint are computed in nonstationary electrical and thermal conditions considering different thermal conductivities and different electrical conductivity laws for the joint material. Results obtained mainly on the tangential field distribution at the dielectric/dielectric interface are discussed. Imposing an electrical conductivity substantially higher in the rubber compared to XLPE has positive impact on the field under the stress cone. However, it is counterbalanced by field enhancement near the central deflector. The strengthening of non-linear effects in the joint contributes to relaxing the field at hot points near the deflector. The impact of thermal conductivity is also evaluated. The results provide orientation for defining appropriate physical properties of joint material for a given cable insulation.

I. INTRODUCTION

Cable terminations and joints are the least reliable components of a HV cable system due to the complexity of their electrical, thermal and mechanical design [1], [2]. The choice of rubber material used in DC accessories as joints is a delicate task as the stresses to support resort to both capacitive (short time, impulse) and resistive (steady state) field distribution, and the thermal gradient set during cable operation further modifies the stress distribution. For HVDC accessories of cables with synthetic insulation, typically two kinds of joint materials are used, which are Ethylene-Propylene-Diene monomer (EPDM) and Silicone rubber (SiR) [2]. Their chemical nature is very different and their physical properties too. SiR tends to have higher electrical conductivity and lower thermal conductivity than EPDM, but compounding may greatly change these properties.

Because accessories work in complex situation, with thermal gradient combined to axial and longitudinal electric stress, optimizing material to define the 'ideal' electrical properties is not an easy task. We have computed the field distributions in a model of HVDC joint (cf. Fig. 1) obtained under nonstationary electrical conditions and different thermal conditions considering known properties of EPDM and SiR and HVDC-grade cross-linked polyethylene (XLPE) as cable insulation [3], [4]. The field distribution at short stressing time is governed by the permittivity of the insulations, while at long time it is

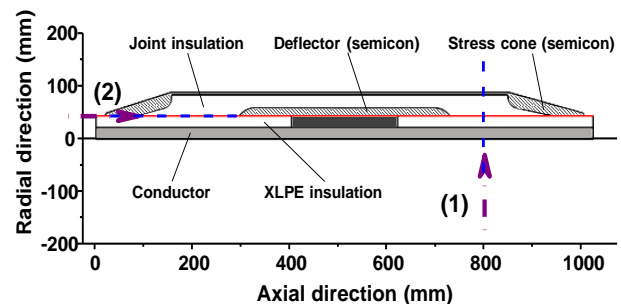


Fig. 1. Scheme of the joint. (1) and (2) define cuts along which tangential field and radial field are represented in the following. White: insulations; Hatched area: semicon; Light grey: conductor; Dark grey: heat distributor.

controlled by the electrical conductivity which is dependent on temperature and electric field.

The distribution of the electric field along the radial direction (1) of the joint (Fig. 1) is relatively easy to anticipate as it results directly from the change in conductivity vs. radius. Besides, the interface between cable insulation and joint insulation constitutes a weak point of the accessory. Then, the tangential electric field along direction (2) is of particular interest. Its variation is more difficult to anticipate than the radial field. We have shown that the axial contribution of the field under the stress cone is significantly reduced when the electrical conductivity of the joint increases [3], [4]. It seems due to a move of the field into the cable insulation followed by a redirection of the field lines to the radial direction. Our purpose in this contribution is to complete our understanding of the distribution of the tangential field considering different thermal conductivities for the joint material and investigating the consequence of having a strong non-linear conductivity in the joint material. Indeed, the joint design can be achieved with inserting non-linear material along the interface that distributes the field homogeneously [5], or designing the joint material such that non-linearity and field grading are operant [6].

II. MODEL HYPOTHESES

Fig. 2 shows the conductivity versus field at two temperatures obtained by measurement for the XLPE and the EPDM. Dotted lines are experimental data obtained on XLPE and on EPDM. Experimental data were fitted using an equation of the form:

$$\sigma_3(T, E) = A \cdot \exp\left(-\frac{E_a}{kT}\right) \cdot \frac{\text{sh}(\beta_E(T) \cdot E)}{E^a} \quad (1)$$

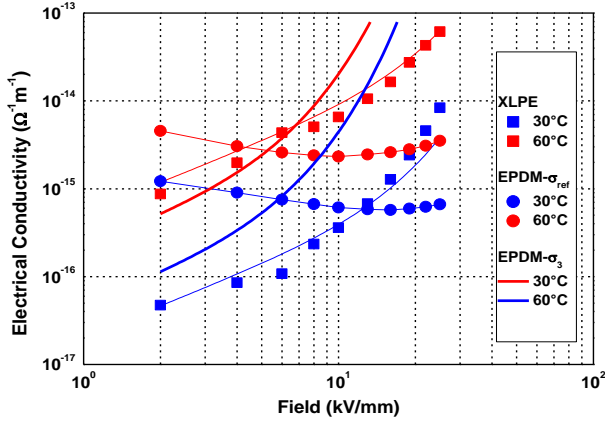


Fig. 2. Field dependence of the electrical conductivity of XLPE, EPDM and EPDM with new conductivity law at 30 and 60°C. Symbols: experimental data; lines: fit to (1). Bold lines are conductivity laws for Case 3.

TABLE I
THERMAL AND ELECTRICAL PARAMETERS FOR INSULATING MATERIALS.

	XLPE	EPDM
Relative permittivity ϵ_r	2.30	2.90
Thermal conductivity λ (W/m/K)	0.38	0.30
Specific heat c_p (J/g/K)	1.90	0.73
Electrical conductivity:		
σ (S/m) at 30°C, 2 kV/mm	4.7×10^{-17}	1.0×10^{-15}
Temperature coefficient E_a (eV)	1.0	0.44
Field coefficient β_E (m/V)	1.38×10^{-7}	0.95×10^{-7}
	at 60°C	1.12×10^{-7}
Field power factor a	-0.15	1.42

with the model parameters defined in Table I. Here, k is the Boltzmann's constant, A is a pre-exponential factor that relates to the conductivity at reference temperature and field. The field distribution was modeled considering a stress cycle in which a voltage of +200 kV is applied for 24 h. Then the joint is grounded and a negative voltage of -200 kV is applied for 24 h.

The thermal conditions were either isotherm at 30°C or a thermal gradient set by injecting a current of 1 kA in the conductor. The modelling is achieved using Comsol Multiphysics® in non-stationary conditions, thermally (initial

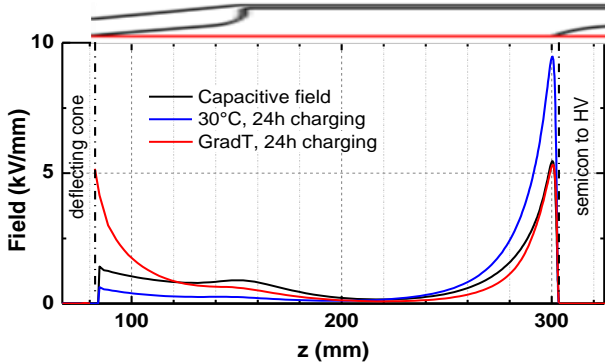


Fig. 3. Tangential field distributions at the XLPE/EPDM interfaces at short time (capacitive distribution) and in quasi-steady state: at 30°C and under thermal gradient. The top of the figure is a drawing of the joint materializing the position in respect to the cone (left) and the deflector.

temperature is 30°C) and electrically. Details of the physical modelling are given in [3].

For a temperature of 30°C, the conductivity in the EPDM is much larger than that in XLPE. As a consequence, the field is moved to the insulation and the tangential field under the cone is low, see Fig. 3. The same feature holds in any thermal condition for a conductivity larger than that of XLPE and nearly field-independent [4].

As a consequence of the reduction of the tangential field under the cone, a strengthening of the field near the central deflector is obtained (resulting from a redistribution of the voltage between the stress cone and the deflector). However, the effects depend on the local temperature and on the respective laws adopted for the conductivity variation with temperature and field. In order to sort out the role of the different factors, two additional case studies are treated and compared in this work:

- Case 1: reference (see Table I and σ_{ref} in Fig. 2);
- Case 2: reduced thermal conductivity for EPDM, $\lambda = 0.20$ W/m/K, the other parameters being those of Table I;
- Case 3: different law for the conductivity, i.e. $\beta_E = 4.0 \times 10^{-7}$ m/V and $\sigma(30^\circ\text{C}, 2 \text{ kV/mm}) = 1.0 \times 10^{-16}$ S/m, the other parameters being those of Table 1. The field dependencies of the conductivity are plotted as solid lines (σ_3) for temperatures of 30 and 60°C in Fig. 2.

III. RESULTS AND DISCUSSION

A. Temperature distribution

The thermal conductivity of the EPDM has a significant impact on the temperature distribution in the joint. Fig. 4 depicts this distribution along the lines (1) and (2) of Fig. 1. In the steady state, the temperature at XLPE/conductor interface is 6°C larger (78 vs 72°C) than in Case 2. Not only a higher temperature, also a larger thermal gradient through the insulation appears. Regarding the temperature at the interface, also a significant difference appears when changing the thermal conductivity, with an increase by up to 7°C with the lower conductivity. The temperature under the cone is lower than in the rest of the interface and the difference is more important for the lower thermal conductivity (Case 2).

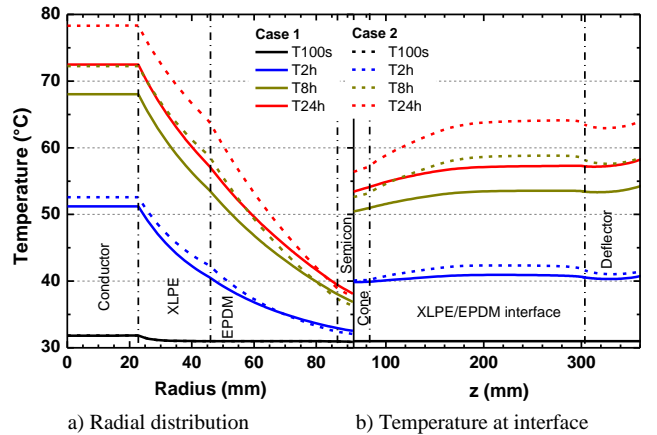
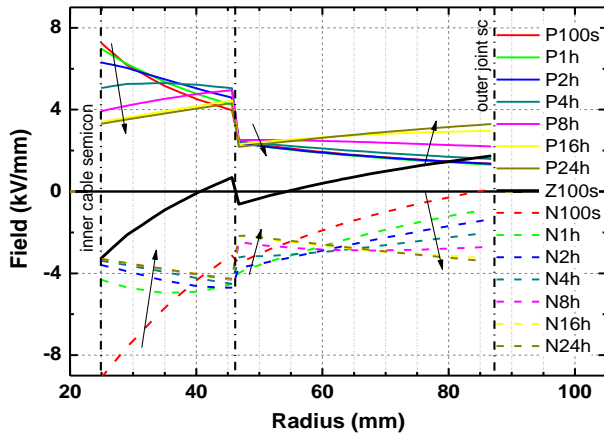


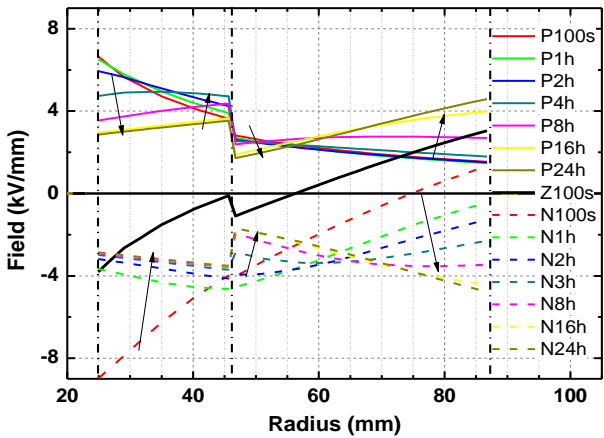
Fig. 4. Temperature profiles up to quasi-steady state (24 h) along directions (1) and (2) of Fig. 1 when injecting 1 kA in the conductor. Case 1: reference; Case 2: low thermal conductivity.

B. Field distributions

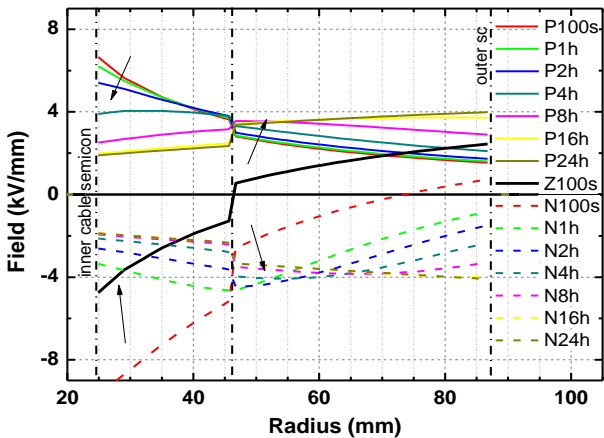
The radial and tangential field distributions at different times during the stress cycle for the different case studies are plotted in Fig. 5 and 6, respectively. The arrows indicate the evolution of the field with time. The temperature rises during ≈ 16 h.



a) Case 1: Reference conditions



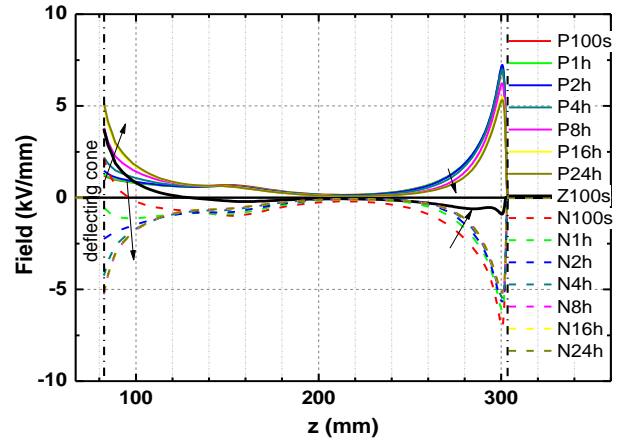
b) Case 2: Low thermal conductivity



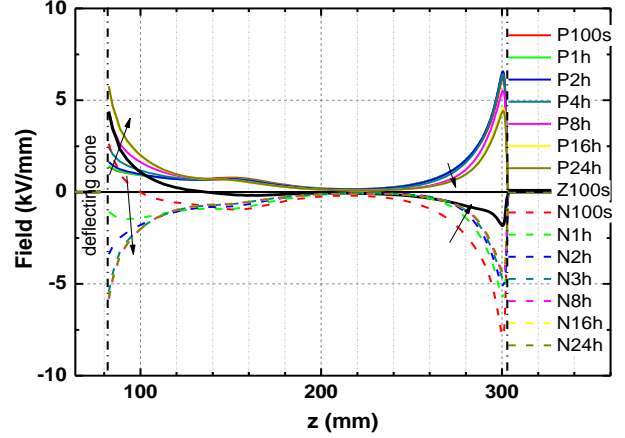
c) Case 3: Enhanced field grading

Fig. 5. Radial field distribution in the XLPE/EPDM joint along line (1), Fig. 1 at different times after voltage application (200 kV followed by voltage polarity inversion) for different physical parameters. The cable is initially at 30°C and a current of 1 kA is injected at the same time as the voltage is applied. Vertical lines indicate the boundaries of the insulators. The curves in black correspond to the set to 0 V after 24 h at +200 kV. Arrows indicate trends for field variation with time.

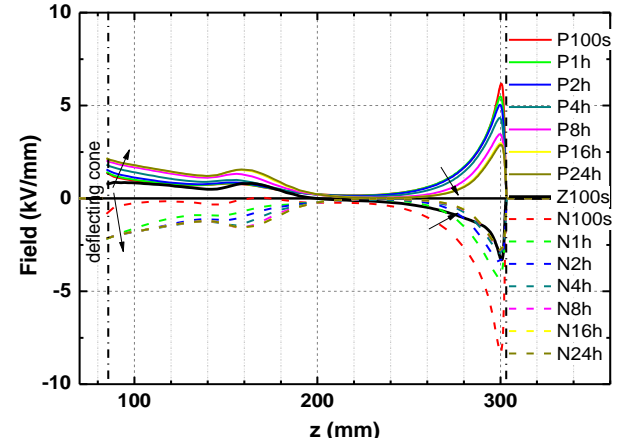
For the radial field distribution, Fig. 5a, a stress inversion phenomenon occurs with time, due to conductivity gradient. The field moves from the capacitive distribution to a resistive one and the field stays higher in the XLPE due to a lower permittivity in XLPE than in EPDM and of a lower conductivity



a) Case 1: Reference conditions



b) Case 2: Low thermal conductivity



c) Case 3: Enhanced field grading

Fig. 6. Axial field distribution at the XLPE/EPDM interface along line (2), Fig. 1 at different times after voltage application (200 kV followed by voltage polarity inversion) for different physical parameters.

Vertical lines define insulator boundaries. The curves in black correspond to the set to 0 after 24 h at +200 kV.

Ground on the left; HV on the right.

Arrows indicate trends for field variation with time.

in the considered temperature / field ranges (Fig. 2 and 4). Increasing the thermal conductivity, Fig. 5b, has as main effect to increase the stress inversion phenomenon, especially in the EPDM material, where the thermal gradient is increased.

With the modified conductivity law, Fig. 5c, the stress inversion process is still observed but it is milder than for Case 1 due to the stress grading introduced by the new conductivity law. The field is getting more homogenous in the material. However, this goes with a larger over-stress at voltage polarity reversal.

Regarding now the behavior of the tangential field at the interface, Fig. 6, it can be seen that the change in thermal conductivity does not have a great impact. The field increases with time at the stress cone and decreases at the deflector side. Considering the residual field at the passage to 0 V, the variations are slightly larger in Case 2. In fact, considering Fig. 2, the values of conductivity for a temperature of 60°C and field of ≈ 5 kV/mm are close for the different materials/cases.

Changing the electrical conductivity law appears to have greater impact, Fig. 6c. The field spreads more along the interface, in such a way that the maximum tangential field does not exceed 3 kV/mm in steady state. The shape of the profiles approaches those found when considering a full joint made of XLPE [4]. The trend could be expected considering the parallel behavior of the electrical conductivities at low field and high temperature for XLPE and EPDM-Case 3, cf. Fig. 2.

The simulations achieved are based on an existing conductivity law established for XLPE and attempt to smooth the field in the joint by adjusting the properties of the joint material. Already, the XLPE conductivity is substantially non-linear. The laws previously considered in [3], [4] were with lower non-linearity. The steeper-than XLPE non-linearity as used in Case 3 does not provide great improvement in the field distribution, compared to pure XLPE. Large field grading effects are attainable in field-grading layers with filled polymers [7]; the difficulty is to keep a relatively low field conductivity and a low threshold field.

Regarding the thermal conductivity effect, the main consequence is an increase in the device temperature and temperature gradient. As a result, the stress inversion phenomenon is stronger as seen in the radial field distribution. The consequences on the tangential field distribution are mild.

IV. CONCLUSION

The field distribution in model HVDC joint has been investigated by simulation under non-stationary electrical and thermal conditions and considering different properties of the joint material. The following conclusions can be drawn, particularly regarding the tangential field distribution:

- the conductivity dependence on field and temperature of the joint material is to be adapted to that of the cable insulation;
- moving the field to the XLPE insulation is efficient to reduce the tangential field under the stress cone. However, the field is reported to the deflector which may lead to overstress. Therefore, the conductivity in the joint material should not exceed significantly that of the cable insulation;
- it is important to develop non-linearity in the joint material larger than that of the cable insulation in order to reach a nearly constant field under the stress cone and absorb a great part of the potential;
- acting on the temperature dependence of the conductivity along the interface is not likely to lead great improvement in smoothing the field as the axial temperature gradient is mild.

For the future, optimization of material parameters could be achieved defining criteria as maximum field, average field, residual field at grounding, etc. It should go with geometrical optimization of the joint. On the other side, it is important to have at disposal materials with tunable conductivity to optimize joints design.

ACKNOWLEDGMENT

This work is supported by CNRS International Scientific Cooperation Program (PICS) N° PICS07965.

REFERENCES

- [1] H. Ye, T. Fechner, X. Lei, Y. Luo, M. Zhou, Z. Han, H. Wang, Q. Zhuang, R. Xu and D. Li, "Review on HVDC cable terminations", *High Volt.*, vol. 3, pp. 79-89, 2018.
- [2] G. Mazzanti, J. Castellon, G. Chen, J. Fothergill, M. Fu, N. Hozumi, J.H. Lee, J. Li, M. Marzinotto and F. Mauseth, "The insulation of HVDC extruded cable system joints. Part 1: Review of materials, design and testing procedures," *IEEE Trans. Dielectr. Electr. Insul.*, vol. 26, pp. 964–972, 2019.
- [3] T.T.N. Vu, G. Teyssedre and S. Le Roy, "Electric field distribution in HVDC cable joint in non-stationary conditions," *Energies*, vol. 14, 5401 (17pp), 2021.
- [4] G. Teyssedre, T.T.N. Vu and S. Le Roy, "Electric field distribution in HVDC cable joint in non-stationary conditions," *Proc. 2021 IEEE 13th International Conference on the Properties and Applications of Dielectric Materials (ICPADM)*, 2021, pp. 406-409.
- [5] H. Ghorbani, M. Jeroense, C. Olsson and M. Saltzer, "HVDC cable systems—Highlighting extruded technology," *IEEE Trans. Power Delivery*, vol. 29, pp. 414-421, 2014.
- [6] S. Hou, M. Fu, C. Li, B. Han, C. Zhang and Z. Li, "Electric field calculation and analysis of HVDC cable joints with nonlinear materials," *Proc. 2015 IEEE 11th International Conference on the Properties and Applications of Dielectric Materials (ICPADM)*, 2015, pp. 184-187.
- [7] M. Pradhan, H. Greijer, G. Eriksson and M. Unge, "Functional behaviors of electric field grading composite materials," *IEEE Trans. Dielectr. Electr. Insul.*, vol. 23, pp. 768-778, 2016.